

## Heavy baryon spectroscopy from the lattice

K. C. Bowler, R. D. Kenway, O. Oliveira, D. G. Richards, and P. Ueberholz\*  
*Department of Physics and Astronomy, The University of Edinburgh, Edinburgh EH9 3JZ, Scotland*

L. Lellouch,<sup>†</sup> J. Nieves,<sup>‡</sup> C. T. Sachrajda,<sup>§</sup> N. Stella, and H. Wittig<sup>||</sup>  
*Physics Department, The University, Southampton SO17 1BJ, United Kingdom*

(UKQCD Collaboration)

(Received 5 February 1996)

The results of an exploratory lattice study of heavy baryon spectroscopy are presented. We have computed the full spectrum of the eight baryons containing a single heavy quark, on a  $24^3 \times 48$  lattice at  $\beta=6.2$ , using an  $O(a)$ -improved fermion action. We discuss the lattice baryon operators and give a method for isolating the contributions of the spin doublets  $(\Sigma, \Sigma^*)$ ,  $(\Xi', \Xi^*)$ , and  $(\Omega, \Omega^*)$  to the correlation function of the relevant operator. We compare our results with the available experimental data and find good agreement in both the charm and the  $b$ -quark sectors, despite the long extrapolation in the heavy quark mass needed in the latter case. We also predict the masses of several undiscovered baryons. We compute the  $\Lambda$ -pseudoscalar meson and  $\Sigma$ - $\Lambda$  mass splittings. Our results, which have errors in the range 10–30%, are in good agreement with the experimental numbers. For the  $\Sigma^*$ - $\Sigma$  mass splitting, we find results considerably smaller than the experimental values for both the charm and the  $b$ -flavored baryons, although in the latter case the experimental results are still preliminary. This is also the case for the lattice results for the hyperfine splitting for the heavy mesons. [S0556-2821(96)00117-8]

PACS number(s): 14.20.Mr, 12.38.Gc, 12.39.Hg

### I. INTRODUCTION

The discovery of the  $\Lambda_b$  baryon at the CERN  $e^+e^-$  collider LEP [1] and the claims of indirect evidence for  $\Lambda_b$  and  $\Xi_b$  semileptonic decays [2] have triggered an increased interest in the spectroscopy and weak decays of heavy baryons. The interest in the spectroscopy, in particular, has been considerably boosted after the announcement of the discovery of several spin- $\frac{3}{2}$  charm and  $b$ -flavored baryons [3,4].

The properties of hadrons containing a heavy quark can be studied using lattice QCD calculations, which provide nonperturbative, model-independent results. Experience gained through studies of heavy mesons has provided the framework for an investigation of the phenomenology of heavy baryons. Furthermore, the study of the spectrum of heavy baryons is a necessary precondition for the measurement of the weak matrix elements of semileptonic decays of  $b$ -flavored baryons. The computed masses and matrix elements can then be combined with an analysis carried out in heavy quark effective theory (HQET) [5,6] to extract an in-

dependent measurement of the Cabibbo-Kobayashi-Maskawa (CKM) matrix elements  $V_{cb}$  and  $V_{ub}$ .

The subject of spectroscopy has been widely discussed in the literature, mainly using potential models [7], HQET [8], or a combination of the latter with chiral perturbation theory [9]. Recently, there have been attempts to compute the mass of the  $\Lambda_h$  (one heavy quark and two light quarks) [10] and of the  $\Xi_{hh}$  (two heavy quarks and one light quark) on the lattice [11]. In this paper, for the first time, the full spectrum of the lowest-lying baryons containing one heavy quark is computed. In particular, we define operators suitable for the simulation of baryon spin doublets with total spin  $\frac{1}{2}$  and  $\frac{3}{2}$ , such as the  $(\Sigma, \Sigma^*)$ ,  $(\Xi', \Xi^*)$ , and  $(\Omega, \Omega^*)$ . The quality of the signal we have observed and the agreement of our estimates with the available experimental data are good, thus giving us confidence in the reliability of our predictions.

The quark content and quantum numbers of the baryons we have considered are summarized in Table I. On the lattices available at present, it is not possible to simulate directly the  $b$  quark, whose mass is larger than the cutoff. Therefore, we have computed four heavy quark masses around that of the charm quark and interpolated (extrapolated) the results to the charm ( $b$ ) quark, relying on the predictions of HQET. The masses of the charm and  $b$  quark were fixed from the masses of the  $D$  and  $B$  mesons, respectively. The results of the extrapolation in the heavy quark mass, could be checked carefully, given the relatively large sample of masses available. On the other hand, we have only used two different values of the light quark mass, thus limiting our ability to perform a detailed analysis of the chiral behavior. Our results for the masses are given in Table II, where the first set of errors is purely statistical and the sec-

\*Present address: Department of Physics, University of Wuppertal, Wuppertal D-42097, Germany

<sup>†</sup>Permanent address: Centre de Physique Théorique, CNRS Luminy, Case 907, F-13288 Marseille Cedex 9, France.

<sup>‡</sup>Permanent address: Departamento de Física Moderna, Universidad de Granada, 18071, Spain.

<sup>§</sup>Address from 1 Oct. 1995 to 1 Oct. 1996: Theory Division, CERN, 1211 Geneva 23, Switzerland.

<sup>||</sup>Present address: DESY-IFH, Platanenallee 6, D-15738 Zeuthen, Germany.

TABLE I. Summary of the quantum numbers of the eight baryons containing a single heavy quark.  $I$ ,  $s_l^{\pi_l}$  are the isospin and the spin parity of the light degrees of freedom and  $S$ ,  $J^P$  are the strangeness and the spin parity of the baryon.

Baryon	( $S$ )	$J^P$	( $I$ )	$s_l^{\pi_l}$	Quark content	Operator
$\Lambda_{c,b}$	(0)	$\frac{1}{2}^+$	(0)	$0^+$	$(ud)c,b$	$\mathcal{O}_5$
$\Sigma_{c,b}$	(0)	$\frac{1}{2}^+$	(1)	$1^+$	$(uu)c,b$	$\mathcal{O}_\mu$
$\Sigma_{c,b}^*$	(0)	$\frac{3}{2}^+$	(1)	$1^+$	$(uu)c,b$	$\mathcal{O}_\mu$
$\Xi_{c,b}$	(-1)	$\frac{1}{2}^+$	( $\frac{1}{2}$ )	$0^+$	$(us)c,b$	$\mathcal{O}_5$
$\Xi'_{c,b}$	(-1)	$\frac{1}{2}^+$	( $\frac{1}{2}$ )	$1^+$	$(us)c,b$	$\mathcal{O}'_\mu$
$\Xi_{c,b}^*$	(-1)	$\frac{3}{2}^+$	( $\frac{1}{2}$ )	$1^+$	$(us)c,b$	$\mathcal{O}'_\mu$
$\Omega_{c,b}$	(-2)	$\frac{1}{2}^+$	(0)	$1^+$	$(ss)c,b$	$\mathcal{O}_\mu$
$\Omega_{c,b}^*$	(-2)	$\frac{3}{2}^+$	(0)	$1^+$	$(ss)c,b$	$\mathcal{O}_\mu$

ond set is an estimate of the systematic uncertainty in the calibration of the lattice spacing. Our results are in good agreement with the experimental determinations, where available.<sup>1</sup> We also present estimates for the  $\Lambda$ -pseudoscalar meson mass splittings. Our results are

$$\frac{M_{\Lambda_c} - M_D}{M_{\Lambda_c} + M_D} = 0.099^{+9}_{-7} \quad \frac{M_{\Lambda_b} - M_B}{M_{\Lambda_b} + M_B} = 0.033^{+5}_{-4} \quad (1)$$

to be compared with the experimental values<sup>2</sup>

$$\frac{M_{\Lambda_c} - M_D}{M_{\Lambda_c} + M_D} = 0.100(3) \quad \frac{M_{\Lambda_b} - M_B}{M_{\Lambda_b} + M_B} = 0.033(5). \quad (2)$$

Similarly, for the  $\Sigma$ - $\Lambda$  splitting, we find

$$\frac{M_{\Sigma_c} - M_{\Lambda_c}}{M_{\Sigma_c} + M_{\Lambda_c}} = 0.039^{+9}_{-9} \quad \frac{M_{\Sigma_b} - M_{\Lambda_b}}{M_{\Sigma_b} + M_{\Lambda_b}} = 0.017^{+5}_{-7} \quad (3)$$

which compare well with the experimental numbers

$$\frac{M_{\Sigma_c} - M_{\Lambda_c}}{M_{\Sigma_c} + M_{\Lambda_c}} = 0.035(1) \quad \frac{M_{\Sigma_b} - M_{\Lambda_b}}{M_{\Sigma_b} + M_{\Lambda_b}} = 0.016(2). \quad (4)$$

The last number in Eq. (4), extracted from the data presented in Ref. [4], is still preliminary.

We also make a first attempt to estimate the spin splitting of the doublets ( $\Sigma^*$ ,  $\Sigma$ ), ( $\Xi^*$ ,  $\Xi'$ ), and ( $\Omega^*$ ,  $\Omega$ ) by isolating the contributions which the two particles give to the same correlation function. We find small, negative splittings, which, in most cases, become compatible with zero after the extrapolations because of the increased statistical errors. The

<sup>1</sup>The experimental evidence for the  $\Xi'_c$  baryon is based on a collection of 11 events, and no estimate of the statistical error is given, see Ref. [12]. We note that the physical  $\Xi'_h$  and  $\Xi_h$  states are mixtures of the states which we measure here, where the light-quark system has definite spin. It has been argued that such mixing [13] becomes negligible in the heavy-quark limit [8,9]. See the conclusions for further comments.

<sup>2</sup>Errors on the experimental data are added in quadrature.

simple quark model expectation is that the splittings are positive, although some of the experimental data are still inconclusive. If this expectation is confirmed by experiment, we could be facing a situation similar to that of the hyperfine splitting in heavy meson systems, where the splitting is underestimated using both the standard Wilson action and the Sheikholeslami-Wohlert (SW) action [14]. The meson hyperfine splitting is sensitive to the chromomagnetic moment term which appears at  $\mathcal{O}(a)$  in improved fermion actions [15]. We plan to investigate the sensitivity of the baryon hyperfine splitting by using the tadpole-improved Sheikholeslami-Wohlert action [16].

This paper is organized as follows. In Sec. II we discuss the baryonic operators which have been used in the present study and give details of the simulation. In Sec. III we explain our analysis procedures for the extraction of the masses. The measurement of the mass splittings is reported

TABLE II. Heavy baryons considered in this project. Our results are quoted with a statistical error (first) and a systematic error (second) arising from the uncertainty in the calibration of the lattice spacing. Where available, we report the experimental data.

Baryon	Quark content	$h = \text{charm}$		$h = \text{b quark}$	
		Expt. [MeV]	Latt. [GeV]	Expt. [MeV]	Latt. [GeV]
$\Lambda_h$	$(ud)h$	2285(1)	2.27 <sup>+4 +3</sup> <sub>-3 -3</sub>	5641(50)	5.64 <sup>+5 +3</sup> <sub>-5 -2</sub>
$\Sigma_h$	$(uu)h$	2453(1)	2.46 <sup>+7 +5</sup> <sub>-3 -5</sub>	5814(60)	5.77 <sup>+6 +4</sup> <sub>-6 -4</sub>
$\Sigma_h^*$	$(uu)h$	2530(7)	2.44 <sup>+6 +4</sup> <sub>-4 -5</sub>	5870(60)	5.78 <sup>+5 +4</sup> <sub>-6 -3</sub>
$\Xi_h$	$(us)h$	2468(4)	2.41 <sup>+3 +4</sup> <sub>-3 -4</sub>		5.76 <sup>+3 +4</sup> <sub>-5 -3</sub>
$\Xi'_h$	$(us)h$	2560 <sup>a</sup>	2.57 <sup>+6 +6</sup> <sub>-3 -6</sub>		5.90 <sup>+6 +4</sup> <sub>-6 -4</sub>
$\Xi_h^*$	$(us)h$	2643(2)	2.55 <sup>+5 +6</sup> <sub>-4 -5</sub>		5.90 <sup>+4 +4</sup> <sub>-6 -5</sub>
$\Omega_h$	$(ss)h$	2704(20)	2.68 <sup>+5 +5</sup> <sub>-4 -6</sub>		5.99 <sup>+5 +5</sup> <sub>-5 -5</sub>
$\Omega_h^*$	$(ss)h$		2.66 <sup>+5 +6</sup> <sub>-3 -7</sub>		6.00 <sup>+4 +5</sup> <sub>-5 -5</sub>

<sup>a</sup>For the error on the  $\Xi'_c$  mass, see footnote 1.

in Sec. IV. Our results and the comparison with the physical values are reported in Sec. V. Finally, we present our conclusions.

## II. PARTICLES AND OPERATORS

There are eight lowest-lying baryons containing one heavy and two light quarks (up, down, or strange). The quantum numbers of the charm and  $b$ -flavored baryons are listed in Table I, and their physical masses (see Refs. [3,4,17,18]), are given in Table II. In the context of HQET at lowest order, it is possible to identify the spin-parity quantum numbers of the heavy-quark and of the light-quark system, within each baryon. Furthermore, heavy baryons with common light degrees of freedom exhibit common features; they are expected to be degenerate in mass, and to obey selection rules in weak decays. For example, the hyperfine mass splittings in the doublets  $(\Sigma^*, \Sigma)$ ,  $(\Xi^*, \Xi')$ , and  $(\Omega^*, \Omega)$  are expected to be  $O(1/m_h)$ , where  $m_h$  is the mass of the heavy quark, and the weak semileptonic decay  $\Lambda_b \rightarrow \Sigma_c$  is suppressed since it could only take place if the light-quark system changed quantum numbers.

### A. Operators for heavy baryons

The spectrum of the heavy baryons in Table I can be computed on the lattice by using three interpolating operators

$$\begin{aligned} \mathcal{O}_5 &= \epsilon_{abc} (l^{aT} \mathcal{C} \gamma_5 l'^b) h^c, & \mathcal{O}_\mu &= \epsilon_{abc} (l^{aT} \mathcal{C} \gamma_\mu l'^b) h^c, \\ \mathcal{O}'_\mu &= \epsilon_{abc} (l^{aT} \mathcal{C} \gamma_\mu l'^b) h^c, \end{aligned} \quad (5)$$

where  $a, b, c$  are color indices,  $\epsilon_{abc}$  is the totally antisymmetric Levi-Civita tensor,  $\mathcal{C}$  is the charge conjugation matrix,  $l, l'$  are light quark fields, and  $h$  is the heavy-quark field. The (implicit) spinorial index of the three operators is the (implicit) uncontracted Dirac index carried by the heavy-quark field. By employing the operators in Eq. (5), one creates physical states whose heavy-quark and light-quarks systems have definite quantum numbers, corresponding to the HQET description at lowest order.

The operators in Eq. (5) differ from those used traditionally for the light baryons because of the different flavor quantum numbers. For example, in the case of the  $\Delta$ , which contains three  $u$  valence quarks, the total spin quantum number is guaranteed by the antisymmetry of the wave function. This is no longer true for baryons containing quarks with different flavors, and the projection procedure illustrated below is necessary in order to identify the contribution of both spin- $\frac{1}{2}$  and  $-\frac{3}{2}$  particles.

The operator  $\mathcal{O}_5$  corresponds to  $s_l^{\pi l} = 0^+$  spin parity for the light degrees of freedom and a total spin parity for the baryon  $J^P = 1/2^+$ . The total isospin of the light degrees of freedom is  $I=0$  if  $l=u$  and  $l'=d$ , and  $I=\frac{1}{2}$  if one of the light quarks is the strange quark.

Consider the two-point correlation function  $G_5$ :

$$G_5(\vec{p}, t) = \sum_x e^{-i\vec{p}\cdot\vec{x}} \langle \mathcal{O}_5(\vec{x}, t) \bar{\mathcal{O}}_5(\vec{0}, 0) \rangle. \quad (6)$$

For large time separations, using antiperiodic boundary conditions in the time direction, this becomes, in the continuum limit,

$$\begin{aligned} G_5(\vec{p}, t) &\rightarrow \frac{Z^2}{2E} \{ e^{-Et} (M + \not{p}) - e^{-E(T-t)} (M - \not{\vec{p}}) \} \\ &+ \frac{Z_{PP}^2}{2E_{PP}} \{ e^{-E_{PP}t} (M_{PP} - \not{q}) - e^{-E_{PP}(T-t)} \\ &\times (\not{q} + M_{PP}) \}, \end{aligned} \quad (7)$$

where  $p^\mu = (E, \vec{p})$  is the four-momentum of the baryon and  $\vec{p}^\mu = (E, -\vec{p})$ . In Eq. (7), we have included the contribution of the parity partner (PP) baryon, with four-momentum  $q^\mu = (E_{PP}, \vec{p})$  and  $\vec{q}^\mu = (E_{PP}, -\vec{p})$ . This particle contributes to the correlation function because it has a nonzero overlap with the operator  $\mathcal{O}_5$  given in Eq. (5). At zero momentum, we choose an appropriate combination of spinorial indices such that the baryon, but not the parity partner, propagates forward in time. We find that the amplitude of the parity partner ( $Z_{PP}^2$ ) propagating backward in time is much smaller than that of the forward-propagating baryon ( $Z^2$ ), and, in the following, we will neglect the contribution of the parity partners.

The case of the operator  $\mathcal{O}_\mu$  is more involved than that of  $\mathcal{O}_5$  since it transforms reducibly under the parity-extended Lorentz group. It is the tensor product of a four-vector and a Dirac spinor and thus transforms as  $(1, \frac{1}{2}) \oplus (\frac{1}{2}, 1) \oplus (\frac{1}{2}, 0) \oplus (0, \frac{1}{2})$  [in  $SU(2) \otimes SU(2)$  notation]. It can annihilate/create particles of spin-parity  $\frac{3}{2}^+$  and  $\frac{1}{2}^+$  as well as these particles' parity partners. With the two-point function for the operator  $\mathcal{O}_\mu$  defined as

$$G_{\mu\nu}(\vec{p}, t) = \sum_x e^{-i\vec{p}\cdot\vec{x}} \langle \mathcal{O}_\mu(\vec{x}, t) \bar{\mathcal{O}}_\nu(\vec{0}, 0) \rangle, \quad (8)$$

we find, in the continuum limit, for large values of  $t$  and using antiperiodic boundary conditions in time,

$$\begin{aligned} G_{\mu\nu}(\vec{p}, t) &\rightarrow \frac{Z_{3/2}^2}{2E_{3/2}} e^{-E_{3/2}t} (\not{p}_{3/2} + M_{3/2}) (P^{3/2})_{\mu\nu} (p_{3/2}) \\ &\times \frac{e^{-E_{1/2}t}}{2E_{1/2}} \{ Z_1^2 (\not{p}_{1/2} + M_{1/2}) (P_{11}^{1/2})_{\mu\nu} (p_{1/2}) \\ &- Z_2^2 (\not{p}_{1/2} - M_{1/2}) (P_{22}^{1/2})_{\mu\nu} (p_{1/2}) - Z_1 Z_2 (\not{p}_{1/2} \\ &+ M_{1/2}) (P_{12}^{1/2})_{\mu\nu} (p_{1/2}) + Z_2 Z_1 (\not{p}_{1/2} - M_{1/2}) \\ &\times (P_{21}^{1/2})_{\mu\nu} (p_{1/2}) \} \\ &+ \text{parity partners} - \text{antiparticles}, \end{aligned} \quad (9)$$

where  $p_J^\mu = (E_J, \vec{p})$  and where parity partner contributions are obtained from the original particle contributions with the replacement  $M_J \rightarrow -M_{PP,J}$  while antiparticle contributions are obtained from the original particle and parity partner contributions with the replacement  $M \rightarrow -M$ ,  $\vec{p} \rightarrow -\vec{p}$ , and  $t \rightarrow T-t$  in the exponent. For any given momentum  $p_\mu$ , the

quantities  $(P^{3/2})_{\mu\nu}(p)$  and  $(P_{ij}^{1/2})_{\mu\nu}(p)$ ,  $i, j = 1, 2$ , are the spin projection operators of Ref. [20] and are given by

$$\begin{aligned} (P^{3/2})_{\mu\nu}(p) &= g_{\mu\nu} - \frac{1}{3} \gamma_\mu \gamma_\nu - \frac{1}{3p^2} (\not{p} \gamma_\mu p_\nu + p_\mu \gamma_\nu \not{p}), \\ (P_{11}^{1/2})_{\mu\nu}(p) &= \frac{1}{3} \gamma_\mu \gamma_\nu - \frac{1}{p^2} p_\mu p_\nu + \frac{1}{3p^2} (\not{p} \gamma_\mu p_\nu + p_\mu \gamma_\nu \not{p}), \\ (P_{22}^{1/2})_{\mu\nu}(p) &= \frac{1}{p^2} p_\mu p_\nu, \\ (P_{12}^{1/2})_{\mu\nu}(p) &= \frac{1}{\sqrt{3}p^2} (p_\mu p_\nu - \not{p} \gamma_\mu p_\nu), \\ (P_{21}^{1/2})_{\mu\nu}(p) &= \frac{1}{\sqrt{3}p^2} (\not{p} p_\mu \gamma_\nu - p_\mu p_\nu). \end{aligned} \quad (10)$$

They are orthonormal and idempotent:

$$(P_{ij}^I)_{\mu\rho} (P_{kl}^J)^{\rho\nu} = \delta^{IJ} \delta_{jk} (P_{il}^J)_{\mu}^{\nu}, \quad (11)$$

where  $I, J$  take on values  $\frac{1}{2}$  or  $\frac{3}{2}$ . They satisfy

$$\begin{aligned} \gamma_\mu (P^{3/2})_{\nu}^{\mu} &= 0, \quad p_\mu (P^{3/2})^{\mu\nu} = 0 = (P^{3/2})^{\mu\nu} p_\nu, \\ p_\mu (P_{ij}^{1/2})^{\mu\nu} &= 0 = (P_{ij}^{1/2})^{\mu\nu} p_\nu \quad \text{for } i, j = 1, 2 \end{aligned} \quad (12)$$

and have the useful properties

$$\begin{aligned} \not{p} (P_{ij}^{1/2})^{\mu\nu} &= \pm (P_{ij}^{1/2})^{\mu\nu} \not{p} \text{ for } i = j, - \text{ for } i \neq j, \\ \not{p} (P^{3/2})^{\mu\nu} &= (P^{3/2})^{\mu\nu} \not{p}. \end{aligned} \quad (13)$$

The properties of Eqs. (12) and (13) guarantee that the spin- $\frac{3}{2}$  contribution satisfies the appropriate Rarita-Schwinger equations [21,22] and that the spin- $\frac{1}{2}$  contributions satisfy the appropriate Dirac equations. The diagonal projectors are furthermore complete:

$$g_{\mu\nu} = (P^{3/2})_{\mu\nu}(p) + (P_{11}^{1/2})_{\mu\nu}(p) + (P_{22}^{1/2})_{\mu\nu}(p). \quad (14)$$

To extract the masses of the spin-parity  $\frac{1}{2}^+$  and  $\frac{3}{2}^+$  particles, one needs only to compute the correlators (9) at rest. In this case, the projectors  $P^{3/2}$  and  $P_{11}^{1/2}$  simplify to

$$\begin{aligned} (P^{3/2})^{ij} &= g^{ij} - \frac{1}{3} \gamma^i \gamma^j, \quad i, j = 1, 2, 3, \\ (P_{11}^{1/2})^{ij} &= \frac{1}{3} \gamma^i \gamma^j, \end{aligned} \quad (15)$$

and only act on the spatial components of  $G_{\mu\nu}(\vec{0}, t)$ , i.e.,  $\mu, \nu = 1, 2, 3$ . Since the components corresponding to the other projection operators do not contribute to the spatial components,  $G_{ij}(\vec{0}, t)$ , it is clear from the properties of  $P^{3/2}$  and  $P_{11}^{1/2}$  given in Eqs. (11) and (13) that the  $\frac{3}{2}^+$  contribution can be isolated by considering  $(P^{3/2})^{ij} G_{jk}(\vec{0}, t)$ , and the  $\frac{1}{2}^+$  contribution by considering  $(P_{11}^{1/2})^{ij} G_{jk}(\vec{0}, t)$ . The contributions of forward-propagating parity partners are suppressed by taking suitable combinations of spinorial indices as discussed after Eq. (7) for the case of  $G_5(\vec{0}, t)$ . Those of the

backward-propagating parity partners are naturally smaller because the time intervals over which they propagate are much longer for most values of  $t$  that we consider in analyzing  $G_{jk}(\vec{0}, t)$ . Furthermore, both contributions are again empirically found to be suppressed by the fact that the overlaps of the parity partner states with the operator  $\mathcal{O}^\mu$  are orders of magnitude smaller and their masses slightly larger than those of the original particles.

When space-time is approximated by a hypercubic lattice, full Euclidean O(4) symmetry is reduced to symmetry under the hypercubic group. This reduction means that most irreducible representations of O(4) and its covering group become reducible on the lattice. Fortunately, the representations which concern us here,  $(1, \frac{1}{2})$ ,  $(\frac{1}{2}, 1)$ ,  $(\frac{1}{2}, 0)$ , and  $(0, \frac{1}{2})$ , because of their low dimensionality, remain irreducible on the lattice [35,36,37]. Furthermore, when restricted to the diagonal cubic subgroup (i.e., the lattice analogue of the rotation subgroup),  $(1, \frac{1}{2}) \oplus (\frac{1}{2}, 1)$  decomposes into the reducible representation  $\frac{3}{2} \oplus \frac{1}{2}$  while  $(\frac{1}{2}, 0) \oplus (0, \frac{1}{2})$  reduces to  $\frac{1}{2}$ , where  $\frac{1}{2}$  and  $\frac{3}{2}$  are themselves reductions to the cubic group of continuum spin- $\frac{1}{2}$  and spin- $\frac{3}{2}$  representations. Thus, the space-time transformation properties of the operators  $\mathcal{O}_5$  and  $\mathcal{O}_\mu$  on the lattice are analogous to what they are in the continuum. Moreover, using the results of Ref. [35], one can show that the cubic representations  $\frac{1}{2}$  and  $\frac{3}{2}$  mix only with the continuum spins

$$\left( \frac{1}{2} \right)_{\text{cubic}} : \frac{1}{2}, \frac{7}{2}, \frac{9}{2}, \dots \left( \frac{3}{2} \right)_{\text{cubic}} : \frac{3}{2}, \frac{5}{2}, \frac{7}{2}, \dots \quad (16)$$

Therefore, if one isolates correctly the cubic  $\frac{1}{2}$  and  $\frac{3}{2}$  contributions to  $G_{\mu\nu}(\vec{p}, t)$ , one isolates unambiguously the contributions of the continuum spin- $\frac{1}{2}$  and spin- $\frac{3}{2}$  states in the large time limit (assuming, of course, that higher spin states are more massive). It should be emphasized that this isolation of the cubic representations must be done carefully because it is not known, *a priori*, which of the spin- $\frac{1}{2}$  or the spin- $\frac{3}{2}$  states is more massive. Fortunately, at zero momentum the continuum rest frame projectors given in Eq. (15) are sufficient because they implement the Clebsch-Gordan decomposition of the product representation spin-1  $\otimes$  spin- $\frac{1}{2}$  into spin- $\frac{1}{2}$  and spin- $\frac{3}{2}$ , a decomposition which survives the reduction of SU(2) to the double-valued cubic subgroup because irreducible representations of SU(2) with spin less than or equal to  $\frac{3}{2}$  are irreducible when reduced to that subgroup. It should further be noted that properties of operators and states under parity transformations are unaffected by the discretization of space-time.

A similar discussion applies to the operator  $\mathcal{O}'_\mu$ . In fact, the structure of the corresponding correlator in terms of quark propagators is the same as that of  $\mathcal{O}_\mu$ ; the only effect of the additional Wick contraction in the  $\mathcal{O}_\mu$  correlator is to change the overall normalization.

Thus, we have shown in the present section how to isolate the contributions of different physical baryon states to the two-point functions of Eqs. (7) and (9). In the following sections we shall use these procedures to determine the heavy-light baryon spectrum. To improve the overlap of the interpolating operators  $\mathcal{O}_5$ ,  $\mathcal{O}_\mu$ , and  $\mathcal{O}'_\mu$  with the corre-

sponding physical baryon states, we smear these operators as described in the Appendix. Though this smearing further complicates the isolation of various physical baryon state contributions for nonzero two-point function momentum  $\vec{p}$  (please refer to the Appendix for details), the baryon spectrum that we obtain here only requires an analysis of zero-momentum, smeared two-point functions to which the discussion of the present section applies unchanged.

### B. Details of the simulation

Our calculation is performed on 60 SU(3) gauge field configurations generated on a  $24^3 \times 48$  lattice at  $\beta = 6.2$ , using the hybrid overrelaxed algorithm described in Ref. [19]. The quark propagators were computed using the  $O(a)$ -improved Sheikholeslami-Wohlert action, which is related to the standard Wilson fermion action via

$$S_F^{SW} = S_F^W - i \frac{\kappa}{2} \sum_{x,\mu,\nu} \bar{q}(x) F_{\mu\nu}(x) \sigma_{\mu\nu} q(x), \quad (17)$$

where  $\kappa$  is the hopping parameter. The use of the SW action reduces discretization errors from  $O(ma)$  to  $O(\alpha_s ma)$  [23,24], which is of particular importance in our study of heavy baryons, where the bare heavy-quark masses are typically around one third to two thirds of the inverse lattice spacing.

The gauge field configurations and light-quark propagators were generated on the 64-node i860 Meiko Computing Surface at the University of Edinburgh. The heavy-quark propagators were computed using the 256-node Cray T3D, also at Edinburgh.

Statistical errors are calculated according to the bootstrap procedure described in [19], for which the quoted errors on all quantities correspond to 68% confidence limits of the distribution obtained from 1000 bootstrap samples.

In order to convert our values for baryon masses and mass splittings into physical units we need an estimate of the inverse lattice spacing in GeV. In this study we take

$$a^{-1} = 2.9 \pm 0.2 \text{ GeV}, \quad (18)$$

thus deviating slightly from some of our earlier papers, where we quoted 2.7 GeV as the central value [19,25,34]. The error in Eq. (18) is large enough to encompass all our estimates for  $a^{-1}$  from quantities such as  $m_\rho$ ,  $f_\pi$ ,  $m_N$ , the string tension  $\sqrt{K}$ , and the hadronic scale  $R_0$  discussed in [27]. This change is partly motivated by a recent study using newly generated UKQCD data [28]; using the quantity  $R_0$  we found  $a^{-1} = 2.95^{+7}_{-11}$  GeV. Also, the nonperturbative determination of the renormalization constant of the axial current yielded a value of  $Z_A = 1.05(1)$  [29] which is larger by about 8% than the perturbative value which we used previously. Thus, the scale estimated from  $f_\pi$  decreases to around 3.1 GeV which enables us to reduce significantly the upper uncertainty on our final value of  $a^{-1}$  [GeV].

Light-quark propagators were computed for quark masses around the strange quark mass, corresponding to hopping parameters  $\kappa = 0.14144$  and  $0.14226$ . Because each heavy baryon contains two light quarks, we can form three baryon correlators for each heavy quark mass, of which two have degenerate light-quark masses and one has nondegenerate

light-quark masses. The masses of the light pseudoscalar meson which are needed for this study, were obtained in Ref. [25]. Results extrapolated to the chiral limit (corresponding to a hopping parameter  $\kappa_{\text{crit}} = 0.14315^{+2}_{-2}$ ) and to the mass of the strange quark ( $\kappa_s = 0.1419^{+1}_{-1}$ ) are also tabulated there.

The heavy-quark propagators have been computed for four values of the heavy-quark mass around that of the charm quark, corresponding to  $\kappa_h = 0.133, 0.129, 0.125,$  and  $0.121$ . The masses of the heavy-light pseudoscalar mesons can be found in Ref. [34].

In order to enhance the signal for the baryon correlation functions, the light- and heavy-quark propagators have been computed using the Jacobi smearing method, [30] either at the source only (SL) or at both the source and the sink (SS). Since smearing is not a Lorentz-invariant operation, it might alter some of the transformation properties of nonscalar observables. We have found that such an effect is evident in the baryonic correlators at nonzero momentum, and we present the results of a study of these effects in the Appendix. This issue, which does not affect the spectrum, represents an important new effect which is crucial in the extraction of the amplitude  $Z$ , and, therefore, in the measurement of the weak matrix elements entering the semileptonic decays of the  $\Lambda_b$ .

### III. ANALYSIS DETAILS

It follows from Eq. (7) that, for  $t > 0$ ,

$$\begin{aligned} [G_5(\vec{0}, t)]_{11} &= [G_5(\vec{0}, t)]_{22} = -[G_5(\vec{0}, T-t)]_{33} \\ &= -[G_5(\vec{0}, T-t)]_{44}. \end{aligned} \quad (19)$$

Therefore, we define the  $\Lambda$  correlation function as<sup>3</sup>

$$\begin{aligned} G_\Lambda(t) &= \frac{1}{4} \{ [G_5(\vec{0}, t)]_{11} + [G_5(\vec{0}, t)]_{22} - [G_5(\vec{0}, T-t)]_{33} \\ &\quad - [G_5(\vec{0}, T-t)]_{44} \} \\ &\simeq Z_\Lambda^2 e^{-m_\Lambda t}. \end{aligned} \quad (20)$$

Similarly, for the  $\Sigma$  and  $\Sigma^*$ , we define the correlation functions by taking suitable combinations of the equivalent components, after projection with the operators given in Eq. (15).

#### A. The effective masses

In Fig. 1 we show effective mass plots of the  $\Lambda$  and  $\Sigma$  baryons, in both the SL and SS cases. We compute the effective masses assuming that the correlators' time evolution is given by an exponential:

$$M_{\text{eff}}(t) = \ln \left( \frac{G_{\Lambda, \Sigma}(t)}{G_{\Lambda, \Sigma}(t+1)} \right). \quad (21)$$

<sup>3</sup> $\Lambda$  is a conventional name, by which we mean the baryon whose light quarks are in a  $s^{\pi=0^+}$  state. Depending on the flavor of the latter, this baryon is either the physical  $\Lambda(ud)$  or the  $\Xi(us)$  with spin 0 for the light quarks. A similar convention is used for  $\Sigma$  and  $\Sigma^*$ .

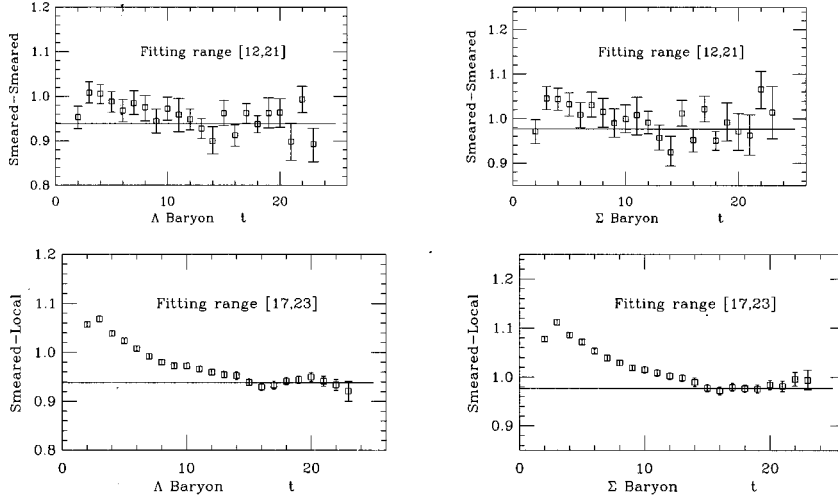


FIG. 1. Effective masses for the  $\Lambda$  and  $\Sigma$  baryons. We show typical plots, corresponding to  $\kappa_h=0.129$  and  $\kappa_{l1}=\kappa_{l2}=0.14144$ . The straight lines are our best fits, which agree for SL and SS correlators starting from  $t_{\min}=17$  onwards.

This is justified since we have checked that the contribution of the parity partners propagating backward in time is completely negligible.

The effective mass is smoother for SL than for SS correlators, because the former are more correlated in time. To establish a fitting range, we fitted the correlators to a single exponential in the range  $[t_{\min}, t_{\max}]$ , where  $t_{\max}$  was fixed at 21 for SS and 23 for SL correlators, and  $t_{\min}$  was varied between 8 and 19. The fits at fixed values of the light and heavy kappas were obtained by minimizing the  $\chi^2$  computed using the full covariance matrix.

As an example, we show in Fig. 2 the results of this analysis for both the  $\Lambda$  and the  $\Sigma$ , with  $\kappa_h=0.129$  and  $\kappa_{l1}=\kappa_{l2}=0.14144$ , for both SS and SL correlators. The behavior of the correlator for the  $\Sigma^*$  baryon is similar, and the features described below are common to all the masses considered in this study.

By considering the  $\chi^2/N_{\text{DF}}$  of the fits, as well as the stability of the results under variation of  $t_{\min}$ , we make the following observations.

(1) The masses obtained from the fits to the SS correlators are stable and the  $\chi^2/N_{\text{DF}}$  are acceptable for  $t_{\min} \geq 11$ . For the SL correlators, the  $\chi^2/N_{\text{DF}}$  are acceptable only for  $t_{\min} \geq 16$ . This behavior supports the hypothesis that by

smearing both the sink and the source one enhances the overlap with the ground state.

(2) The masses obtained from fits to the SL and SS correlators agree around  $t_{\min} \geq 17$ .

(3) As a general feature, we observe that the statistical errors increase with decreasing light-quark mass. This effect is more pronounced for SL than for SS correlators.

The conclusion is that there is a good agreement between SS and SL data, even if, in the latter cases, the plateaus are shorter and the errors slightly larger. Thus, we quote the results obtained by fitting SS correlators in  $t \in [12,21]$ , using those obtained with SL correlators as a consistency check.

## B. Mass extrapolations

We obtain the masses of the eight charm and  $b$ -flavored baryons by extrapolating first in the light-quark masses and then in the heavy-quark mass.

### 1. Extrapolation in the light-quarks system

In order to perform the extrapolation to the chiral limit, we use the three baryon masses obtained from both degenerate (i.e.,  $\kappa_{l1}=\kappa_{l2}=0.14144$ , or 0.14226) and nondegenerate (i.e.,  $\kappa_{l1}=0.14144$  and  $\kappa_{l2}=0.14226$ ) light-quark correlation functions. We assume that, in the chiral regime,  $M_{\text{baryon}}$  depends linearly on the sum of the two light-quark masses, that is,

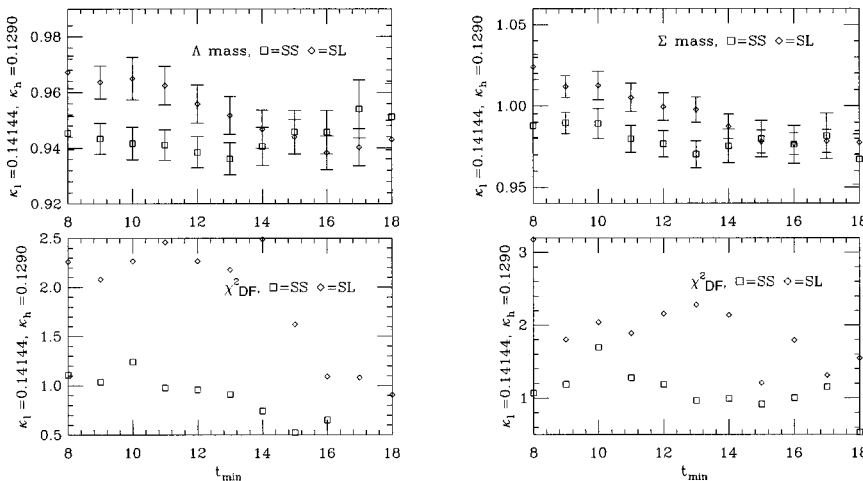


FIG. 2. Masses and  $\chi^2/N_{\text{DF}}$  obtained from a sliding window analysis for the  $\Lambda$  and the  $\Sigma$  baryon correlators.

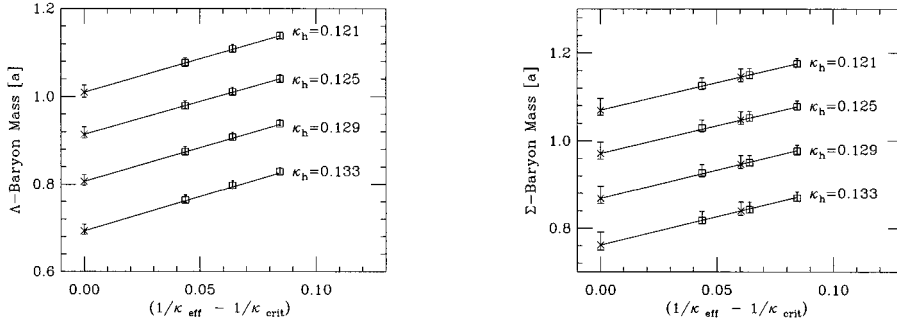


FIG. 3. The chiral behavior of the  $\Lambda$  and  $\Sigma$  masses. The boxes denote data at our three light-quark masses; the crosses denote the extrapolation of our results to the chiral limit and the strange-quark mass.

$$M_{\text{baryon}}(\kappa_h, \kappa_{l1}, \kappa_{l2}) = M_{\text{baryon}}(\kappa_h) + C \left( \frac{1}{2\kappa_{l1}} + \frac{1}{2\kappa_{l2}} - \frac{1}{\kappa_{\text{crit}}} \right) \\ = M_{\text{baryon}}(\kappa_h) + C \left( \frac{1}{\kappa_{\text{eff}}} - \frac{1}{\kappa_{\text{crit}}} \right) \quad (22)$$

with  $\kappa_{\text{eff}}^{-1} = (\kappa_{l1}^{-1} + \kappa_{l2}^{-1})/2$ . This is supported by our data for the masses in the  $\Lambda$  and  $\Sigma$  channels, as shown in Fig. 3, and by previous studies of light meson masses [25,26]. In the  $\Lambda$  channel, extrapolating to  $\kappa_{l1} = \kappa_{l2} = \kappa_{\text{crit}}$ , gives the mass of the  $\Lambda_h$ , while extrapolating  $\kappa_{l1}$  to  $\kappa_{\text{crit}}$  and interpolating  $\kappa_{l2}$  to  $\kappa_s$  gives the mass of the  $\Xi_h$ . Similarly, from the  $\Sigma$  channel we extract the masses of the  $\Sigma_h$ , the  $\Xi'_h$  and the  $\Omega_h$ .

The results of this analysis, obtained from SS correlation functions, are summarized in Table III. By performing the same type of analysis on the SL correlators, we obtained essentially indistinguishable results. We note that the difference in the statistical errors of the SS and SL masses, already present in the fits at fixed  $\kappa$ , is amplified by the extrapolation to the chiral limit. This confirms our earlier conclusion that by using SS data one obtains more precise results.

## 2. Heavy quark extrapolation

The physical masses of the charmed and  $b$ -flavored baryons are obtained by extrapolating the four sets of data, computed at  $\kappa_h = 0.133, 0.129, 0.125$ , and  $0.121$ . In performing these extrapolations, we have been guided by the HQET and have expressed the dependence of the baryon mass  $M_{\text{baryon}}(M_P)$  on the heavy-light pseudoscalar meson mass  $M_P$ , through the following function

$$M_{\text{baryon}}(M_P) = M_P + C + \frac{A}{M_P}, \quad (23)$$

where the two constants  $C$  and  $A$  are the parameters of the fit. The masses of the charm and  $b$ -flavored baryons are obtained for  $M_P = M_D$  or  $M_P = M_B$ , respectively. In Table II we report the results, corresponding to the SS case, in physical units. The numbers corresponding to the charm and  $b$ -quark masses have been obtained assuming  $a^{-1} = 2.9$  GeV. The quoted systematic error arises solely from the uncertainty in the scale and has been estimated by letting  $a^{-1}$  vary by one standard deviation about its central value.

In these fits, the coefficient  $A$ , which quantifies the size of the  $1/m_h$  corrections, is of the expected size, i.e.  $A = O(\Lambda_{\text{QCD}}^2)$ , ranging from about  $(350 \text{ MeV})^2$  to  $(540$

MeV) $^2$ , depending on the particular baryon and on the flavor of the light degrees of freedom. Of course, the  $O(1/m_h)$  corrections play an important role in the case of the mass splittings (see Sec. IV), while they contribute much less to the value of each mass. As a further confirmation of this, we have also set  $A$  to zero and verified that the results of the extrapolation are essentially indistinguishable from those presented in Table II although the  $\chi^2$  are significantly higher. Finally, we have used a function of the kind

$$M_{\text{baryon}}(M_P) = C + A'(M_P - M_0), \quad (24)$$

where a different slope in  $M_P$  is allowed, and we have obtained  $A'$  compatible with 1 in most cases. All of this confirms that heavy-quark symmetry is very well satisfied here. Moreover, the insensitivity of the results to different model-

TABLE III. Masses of the  $\Lambda$ ,  $\Sigma$  and  $\Sigma^*$  in lattice units obtained by fitting the SS correlators in  $t \in [12, 21]$ . Also shown are the corresponding masses after extrapolation in the light-quark masses, using Eq. (22).

$\Lambda$ :				
$\kappa_l$	$\kappa_h = 0.121$	$\kappa_h = 0.125$	$\kappa_h = 0.129$	$\kappa_h = 0.133$
0.14144/0.14144	1.138 $^{+8}_{-7}$	1.040 $^{+9}_{-5}$	0.939 $^{+9}_{-4}$	0.829 $^{+9}_{-4}$
0.14144/0.14226	1.108 $^{+11}_{-6}$	1.011 $^{+11}_{-5}$	0.908 $^{+11}_{-4}$	0.798 $^{+11}_{-4}$
0.14226/0.14226	1.077 $^{+11}_{-7}$	0.979 $^{+12}_{-6}$	0.875 $^{+12}_{-5}$	0.764 $^{+12}_{-5}$
Strange/strange	1.101 $^{+13}_{-9}$	1.002 $^{+13}_{-9}$	0.899 $^{+13}_{-9}$	0.786 $^{+13}_{-9}$
Strange/chiral	1.056 $^{+14}_{-9}$	0.959 $^{+15}_{-7}$	0.853 $^{+14}_{-6}$	0.740 $^{+14}_{-7}$
Chiral/chiral	1.011 $^{+17}_{-13}$	0.913 $^{+16}_{-11}$	0.807 $^{+15}_{-10}$	0.693 $^{+14}_{-10}$
$\chi_{\text{DF}}^2$	0.05	0.3	0.2	0.9
$\Sigma$ :				
$\kappa_l$	$\kappa_h = 0.121$	$\kappa_h = 0.125$	$\kappa_h = 0.129$	$\kappa_h = 0.133$
0.14144/0.14144	1.176 $^{+12}_{-7}$	1.078 $^{+13}_{-6}$	0.977 $^{+14}_{-6}$	0.869 $^{+14}_{-6}$
0.14144/0.14226	1.150 $^{+15}_{-7}$	1.053 $^{+15}_{-7}$	0.950 $^{+17}_{-7}$	0.842 $^{+18}_{-7}$
0.14226/0.14226	1.126 $^{+18}_{-9}$	1.030 $^{+18}_{-9}$	0.927 $^{+19}_{-9}$	0.818 $^{+21}_{-8}$
Strange/strange	1.141 $^{+18}_{-11}$	1.043 $^{+18}_{-10}$	0.941 $^{+18}_{-11}$	0.833 $^{+18}_{-11}$
Strange/chiral	1.108 $^{+22}_{-10}$	1.010 $^{+22}_{-11}$	0.908 $^{+23}_{-11}$	0.801 $^{+25}_{-10}$
Chiral/chiral	1.067 $^{+23}_{-23}$	0.965 $^{+23}_{-12}$	0.862 $^{+23}_{-10}$	0.753 $^{+23}_{-13}$
$\chi_{\text{DF}}^2$	0.8	0.1	1.0	0.7
$\Sigma^*$ :				
$\kappa_l$	$\kappa_h = 0.121$	$\kappa_h = 0.125$	$\kappa_h = 0.129$	$\kappa_h = 0.133$
0.14144/0.14144	1.170 $^{+11}_{-7}$	1.072 $^{+12}_{-7}$	0.969 $^{+12}_{-6}$	0.860 $^{+12}_{-6}$
0.14144/0.14226	1.145 $^{+13}_{-8}$	1.047 $^{+13}_{-8}$	0.944 $^{+14}_{-7}$	0.834 $^{+14}_{-7}$
0.14226/0.14226	1.121 $^{+15}_{-9}$	1.023 $^{+15}_{-9}$	0.920 $^{+16}_{-9}$	0.809 $^{+17}_{-8}$
Strange/strange	1.136 $^{+16}_{-10}$	1.038 $^{+16}_{-10}$	0.934 $^{+16}_{-9}$	0.823 $^{+17}_{-9}$
Strange/chiral	1.104 $^{+18}_{-11}$	1.005 $^{+18}_{-10}$	0.902 $^{+19}_{-10}$	0.791 $^{+20}_{-9}$
Chiral/chiral	1.061 $^{+22}_{-13}$	0.960 $^{+22}_{-12}$	0.856 $^{+22}_{-11}$	0.745 $^{+22}_{-10}$
$\chi_{\text{DF}}^2$	0.4	0.7	0.6	0.5

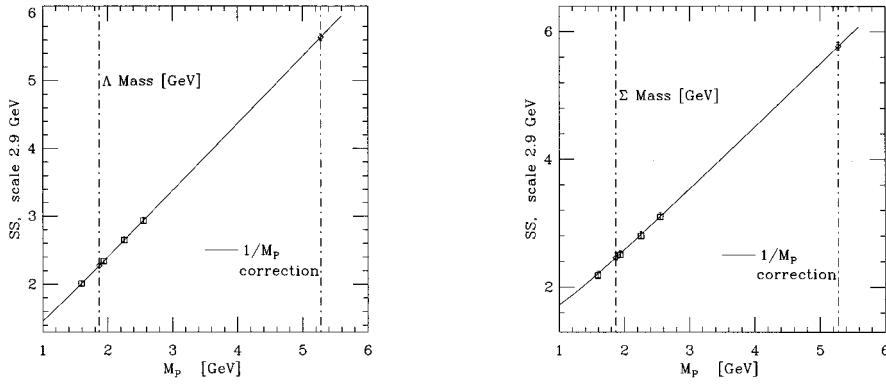


FIG. 4. Extrapolation of the  $\Lambda$  and  $\Sigma$  baryon masses. In the figures both the linear extrapolation and that obtained taking into account  $O(1/M_P)$  correction are shown. The diamonds and crosses correspond to the extrapolations to the charm mass and  $b$ -quark mass, respectively.

ing functions gives us confidence, not only in the interpolation to the charm mass, but also in the long extrapolation to the  $b$ -quark mass. We stress, once more, the total agreement between SS and SL results, both for the final numbers and for the features of the extrapolations. Two examples of the extrapolation to the heavy scale, corresponding to the  $\Lambda$  and the  $\Sigma$ , are shown in Fig. 4.

#### IV. CALCULATION OF MASS SPLITTINGS

Once the value of  $\kappa_h$  is fixed to correspond to the physical quark mass by matching  $M_P$  to either the  $D$ - or the  $B$ -meson mass, no large uncertainties are expected to occur in the measurement of other charm or  $b$ -flavored hadron masses, which are largely determined by that of the heavy quark. On the other hand, splittings in the masses arise from the dynamics of the light quarks and their interactions with the heavy quark. Their study provides a test of HQET as well as important information on the size of various systematic effects.

The mass splittings are small quantities in comparison to the baryon masses themselves. Thus, they are affected by relatively larger statistical errors, as well as being more sensitive to the fitting and extrapolation procedures adopted. Therefore, a particularly careful analysis is required. Once more, we will quote results obtained by fitting SS correlators; the SL correlators give consistent results, although the statistical errors are appreciably larger.

##### A. $\Lambda$ -pseudoscalar meson mass splitting

The  $\Lambda$ -pseudoscalar meson mass splitting is very precisely measured experimentally, especially in the charm sector. Therefore, as we use the pseudoscalar mass to fix the value of the heavy quark  $\kappa$ , the agreement of the lattice value of  $M_\Lambda - M_P$  with experiment reflects the extent to which our calculation properly incorporates the dynamics of the light degrees of freedom. The amount of computational effort devoted to this calculation, both with static [31–33] and propagating Wilson fermions [11] is testimony to its importance. We summarize the results obtained so far [32,33] and compare them with the numbers from this study in Fig. 5.

For the analysis of this splitting, we need the correlation function of the pseudoscalar meson, which was determined in an earlier simulation [34] using the same heavy quarks as this study, but with one additional light quark, corresponding to  $\kappa_l = 0.14262$ . We find that there is very little to be gained

by determining the difference of the masses from the time evolution of the ratio of the  $\Lambda$  and the pseudoscalar meson correlators,<sup>4</sup> as opposed to obtaining it by subtracting the two masses determined separately. One reason is that the statistical errors associated with our measurement of the  $\Lambda$  mass are much larger than those of the pseudoscalar, and would dominate the final uncertainty on the splitting in any procedure. Moreover, when the pseudoscalar correlators were computed, only the heavy-quark propagators were smeared. Here, the light-quark propagators are also smeared, and, consequently, the pseudoscalar and baryon correlation functions suffer from different statistical fluctuations. Therefore, we measure the splitting by taking the difference of the baryon mass, obtained as described in the previous section, and the meson mass, fitted in the range  $t \in [12, 21]$ , as in Ref. [34]. The results, for all the kappa values, are reported in Table IV.

We perform a chiral extrapolation of the mass differences at each heavy  $\kappa$  value. Although we have simulated only two values of the light-quark mass, we have computed baryon correlators corresponding to two degenerate and one nondegenerate case; this last set of data, however, cannot be matched with the mesonic data and cannot be used in the chiral extrapolation. Hence, the chiral extrapolation is modeled by a linear function of the two degenerate light-quark points. Both our results for the  $\Lambda$  extrapolation (see Sec. III) and the evidence reported in Ref. [25] for the meson, justify this procedure.

We performed the extrapolation to the physical pseudoscalar meson masses following two different procedures, in order to have a consistency check (see Fig. 6).

(A) The splittings are first extrapolated in the inverse heavy-quark mass, according to the formula

$$[M_\Lambda - M_P](\kappa_h) = A + \frac{B}{M_P(\kappa_h)} + \frac{C}{M_P^2(\kappa_h)},$$

keeping the light-quark mass fixed. The linear and quadratic extrapolations produce indistinguishable numbers. Then, the two values of this splitting corresponding to the two degen-

<sup>4</sup>Since the behavior of the baryon and meson time slice correlators is different close to the center of the lattice, the ratio method is only safe if one excludes the last few time slices from the fitting range.



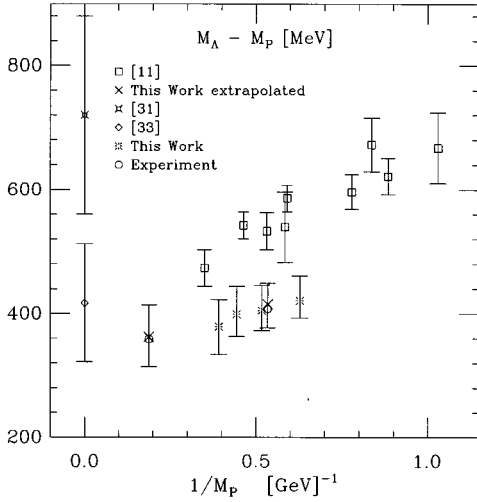


FIG. 5.  $M_\Lambda - M_P$  splitting: comparison of the values obtained by different groups and using different fermion actions. The estimates are also compared with the experimental numbers.

erate light-quark configurations are extrapolated to the chiral limit for each heavy-quark mass.

(B) We employ the reverse procedure in which the mass splittings are first extrapolated to the chiral limit, keeping the heavy-quark mass fixed. The results from the subsequent linear and quadratic extrapolations in the heavy-quark mass are once again compatible.

We conclude that the behavior of the  $\Lambda$ -pseudoscalar splitting is well represented by a linear function of both the light-quark mass and the inverse heavy-quark mass. The results in physical units that we quote in Table V are obtained under this assumption.

### B. $\Sigma$ - $\Lambda$ mass splitting

We have obtained the  $\Sigma$ - $\Lambda$  mass splitting for various  $\kappa$  combinations, both by taking the difference of the fitted masses and by fitting the time evolution of the ratio of  $\Sigma$  and  $\Lambda$  correlators. The numbers obtained with the two methods are in good agreement, but the second procedure yields appreciably smaller errors and is smoother in the chiral limit, proving that it is particularly appropriate when one compares two correlators with a similar structure. The results at each value of the computed masses and after the chiral extrapolation are given in Table VI.

The dependence of the splitting on the heavy-quark mass is extremely weak, suggesting that the  $1/m_h$  corrections to

TABLE IV.  $\Lambda$ -pseudoscalar meson mass splitting, in lattice units, obtained from the difference of the fitted masses.

$\kappa_{11}/\kappa_{12}$	$\kappa_h = 0.121$	$\kappa_h = 0.125$	$\kappa_h = 0.129$	$\kappa_h = 0.133$
0.14144/0.14144	0.212 $^{+7}_{-8}$	0.216 $^{+8}_{-6}$	0.222 $^{+8}_{-5}$	0.229 $^{+8}_{-4}$
0.14226/0.14226	0.173 $^{+10}_{-10}$	0.178 $^{+10}_{-8}$	0.182 $^{+10}_{-7}$	0.189 $^{+10}_{-6}$
Chiral/chiral	0.131 $^{+15}_{-15}$	0.138 $^{+15}_{-12}$	0.140 $^{+14}_{-11}$	0.145 $^{+14}_{-10}$

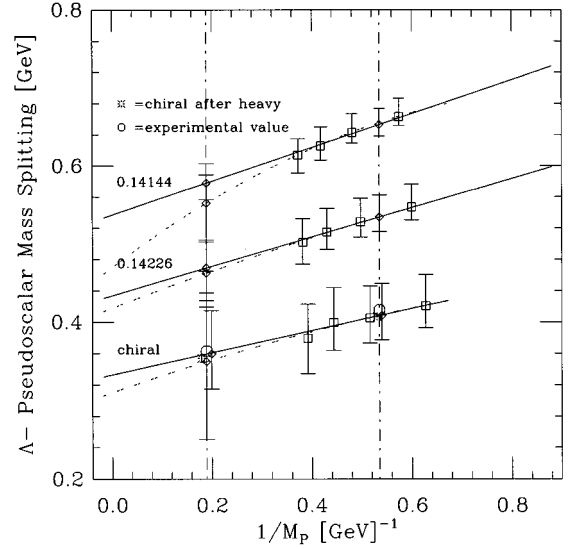


FIG. 6.  $M_\Lambda - M_P$  splitting as obtained adopting the two procedures A and B. The solid lines correspond to the linear extrapolation in the inverse pseudoscalar mass and the dotted line is the same extrapolation modeled with a quadratic dependence. In the plot, the light  $\kappa$  values are also indicated. The results, which are consistent between both methods, are compared with the experimental values. The vertical dotted lines indicate  $1/M_D$  and  $1/M_B$ .

the masses of the two baryons must be very similar and nearly cancel out in the difference. This feature makes it particularly simple to perform the extrapolation to the physical masses, as the fits to linear and quadratic functions of the inverse pseudoscalar meson mass are essentially indistinguishable. This is clearly visible in Fig. 7. We note that our results, presented in Table VII, compare very well with those of the experiment.

### C. Spin splitting

In the HQET, the mass difference within the spin doublets ( $\Sigma, \Sigma^*$ ), ( $\Xi', \Xi^*$ ), and ( $\Omega, \Omega^*$ ) is because of the coupling of the chromomagnetic moment of the heavy quark to the light degrees of freedom. It is, therefore, suppressed by inverse powers of the heavy-quark mass and vanishes in the infinite mass limit.

Because the splitting is such a small effect, it is difficult to measure from our data using either the ratio of the correlators or the difference of the fitted masses. In Figure 8(a) we present the effective mass plot for the ratios of the  $\Sigma^*$  and

TABLE V. Results for the  $\Lambda$ -pseudoscalar splitting, at the physical masses, corresponding to  $a^{-1} = 2.9$  GeV. The two methods illustrated in the text produce essentially identical results, in excellent agreement with the experimental number, given in the last column.

	Procedure A [MeV]	Procedure B [MeV]	Expt. [MeV]
Charm	406 $^{+44}_{-29}$	408 $^{+41}_{-31}$	415(1)
$b$ quark	354 $^{+55}_{-46}$	359 $^{+55}_{-45}$	362(50)

TABLE VI. Estimates of  $M_{\Sigma^*} - M_{\Lambda}$  in lattice units, for various kappa combinations, obtained with the ratio method. The extrapolations are linear, as they were for the masses themselves.

$\kappa_{l1}/\kappa_{l2}$	$\kappa_h = 0.121$	$\kappa_h = 0.125$	$\kappa_h = 0.129$	$\kappa_h = 0.133$
0.14144/0.14144	$(0.37 \begin{smallmatrix} +6 \\ -4 \end{smallmatrix}) \times 10^{-1}$	$(0.36 \begin{smallmatrix} +7 \\ -4 \end{smallmatrix}) \times 10^{-1}$	$(0.37 \begin{smallmatrix} +7 \\ -4 \end{smallmatrix}) \times 10^{-1}$	$(0.37 \begin{smallmatrix} +6 \\ -4 \end{smallmatrix}) \times 10^{-1}$
0.14144/0.14226	$(0.44 \begin{smallmatrix} +7 \\ -8 \end{smallmatrix}) \times 10^{-1}$	$(0.44 \begin{smallmatrix} +8 \\ -7 \end{smallmatrix}) \times 10^{-1}$	$(0.43 \begin{smallmatrix} +8 \\ -7 \end{smallmatrix}) \times 10^{-1}$	$(0.44 \begin{smallmatrix} +8 \\ -6 \end{smallmatrix}) \times 10^{-1}$
0.14226/0.14226	$(0.50 \begin{smallmatrix} +12 \\ -11 \end{smallmatrix}) \times 10^{-1}$	$(0.49 \begin{smallmatrix} +12 \\ -10 \end{smallmatrix}) \times 10^{-1}$	$(0.52 \begin{smallmatrix} +10 \\ -11 \end{smallmatrix}) \times 10^{-1}$	$(0.51 \begin{smallmatrix} +11 \\ -8 \end{smallmatrix}) \times 10^{-1}$
Chiral/strange	$(0.54 \begin{smallmatrix} +15 \\ -15 \end{smallmatrix}) \times 10^{-1}$	$(0.50 \begin{smallmatrix} +17 \\ -13 \end{smallmatrix}) \times 10^{-1}$	$(0.59 \begin{smallmatrix} +13 \\ -15 \end{smallmatrix}) \times 10^{-1}$	$(0.57 \begin{smallmatrix} +14 \\ -10 \end{smallmatrix}) \times 10^{-1}$
Chiral/strange	$(0.65 \begin{smallmatrix} +17 \\ -18 \end{smallmatrix}) \times 10^{-1}$	$(0.65 \begin{smallmatrix} +18 \\ -18 \end{smallmatrix}) \times 10^{-1}$	$(0.67 \begin{smallmatrix} +17 \\ -17 \end{smallmatrix}) \times 10^{-1}$	$(0.66 \begin{smallmatrix} +17 \\ -14 \end{smallmatrix}) \times 10^{-1}$

$\Sigma$  correlation functions (for a heavy quark with  $\kappa_h=0.129$  and for light quarks with  $\kappa_{l1}=\kappa_{l2}=0.14144$ ). It can be seen that the signal is very poor. For this reason we use the difference of the masses obtained by fitting the  $\Sigma^*$  and  $\Sigma$  correlation functions separately as our best estimate for the splitting (this method also leads to a smoother behavior with the mass of the light quarks). In Fig. 8(a) we also plot the splitting obtained in this way.

We present our measurements of the splittings for each  $\kappa$  combination in Table VIII and the extrapolated values at the physical masses in Table VII. They are negative within two standard deviations at fixed light-quark mass, but being affected by large statistical errors, become compatible with zero in the chiral limit. We obtain the splittings at the physical masses, extrapolating in the inverse heavy-quark mass, according to the function

$$[M_{\Sigma^*} - M_{\Sigma}](\kappa_h) = \frac{A}{M_P(\kappa_h)} + \frac{B}{M_P^2(\kappa_h)}. \quad (25)$$

The splitting has been constrained to vanish in the infinite heavy-quark mass limit, as predicted by the HQET. The two extrapolations obtained either by including the quadratic term or by setting  $B=0$  gave essentially indistinguishable results, as can be seen from Fig. 8(b), and good  $\chi^2$ . We also checked the consistency of our data with the predicted behavior, by adding a constant to the function (25), i.e., by allowing the spin splitting to have a nonzero intercept at  $1/M_P=0$ . We find that the values of the intercept are always compatible with zero, being of the order  $-30$  MeV, with errors of about one hundred.

Once more, the results were perfectly consistent. The values presented in Table VII correspond to Eq. (25) with  $B=0$  since this parametrization fits the lattice data very well and makes full use of heavy-quark scaling relations.

TABLE VII. Baryon-pseudoscalar meson and baryon-baryon mass splittings in MeV. The available experimental data are also shown, together with the corresponding references. The experimental errors on the  $\Xi'_c - \Xi_c$  and  $\Xi_c^* - \Xi'_c$  splittings are not published.

	$h = \text{charm}$		$h = \text{b quark}$	
	Expt.	Latt.	Expt.	Latt.
$\Lambda_h - P$	[18] 417(1)	408 $\begin{smallmatrix} +41 & +34 \\ -31 & -33 \end{smallmatrix}$	[18] 362(50)	359 $\begin{smallmatrix} +55 & +27 \\ -45 & -26 \end{smallmatrix}$
$\Sigma_h - \Lambda_h$	[18] 169(2)	190 $\begin{smallmatrix} +50 & +13 \\ -43 & -13 \end{smallmatrix}$	[4] 173(11)	190 $\begin{smallmatrix} +60 & +13 \\ -75 & -13 \end{smallmatrix}$
$\Xi'_h - \Xi_h$	[12] 92	166 $\begin{smallmatrix} +40 & +12 \\ -35 & -13 \end{smallmatrix}$		157 $\begin{smallmatrix} +32 & +11 \\ -64 & -11 \end{smallmatrix}$
$\Sigma_h^* - \Sigma_h$	[19] 77(6)	-17 $\begin{smallmatrix} +12 & +3 \\ -31 & -2 \end{smallmatrix}$	[4] 56(16)	-6 $\begin{smallmatrix} +4 & +1 \\ -11 & -1 \end{smallmatrix}$
$\Xi_h^* - \Xi'_h$	[12] 33	-20 $\begin{smallmatrix} +12 & +2 \\ -24 & -3 \end{smallmatrix}$		-7 $\begin{smallmatrix} +4 & +1 \\ -8 & -1 \end{smallmatrix}$
$\Omega_h^* - \Omega'_h$		-23 $\begin{smallmatrix} +6 & +3 \\ -14 & -2 \end{smallmatrix}$		-8 $\begin{smallmatrix} +2 & +1 \\ -5 & -1 \end{smallmatrix}$

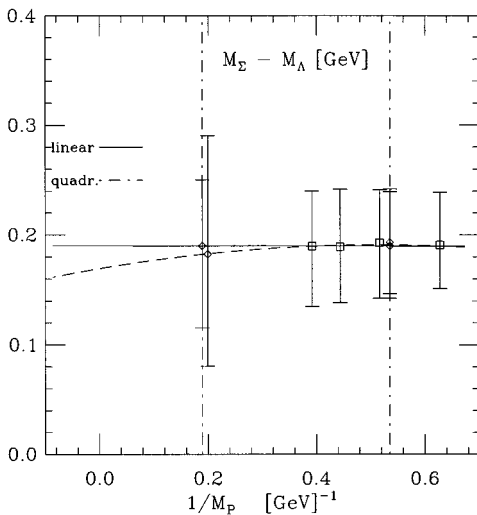


FIG. 7.  $M_{\Sigma^*} - M_{\Lambda}$  as a function of  $1/M_P$ . The linear and the quadratic extrapolations are shown. The vertical dotted lines indicate  $1/M_D$  and  $1/M_B$ , respectively.

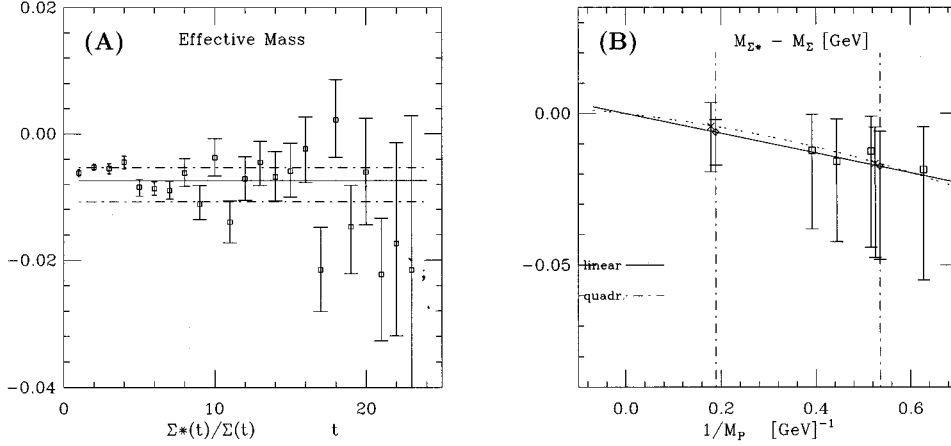


FIG. 8. (a) Effective mass plot for the ratio of correlators  $\Sigma^*(t)/\Sigma(t)$ . The plot corresponds to  $\kappa_{l1} = \kappa_{l2} = 0.14144$  and  $\kappa_h = 0.129$ . The horizontal lines represent the estimate of the mass splitting and the statistical error obtained by taking the difference of the fitted masses. (b)  $M_{\Sigma^*} - M_{\Sigma}$  splitting computed from the mass difference, together with linear and quadratic extrapolations. The vertical dotted lines indicate  $1/M_D$  and  $1/M_B$ .

We note that our value for the  $\Sigma_c^* - \Sigma_c$  splitting is inconsistent with experiment, and in most cases our measured values are consistent with zero. This feature resembles the well-known puzzle of the spin splitting in the mesonic sector [14], whose resolution is believed to lie in a combination of discretization and quenching effects, as argued in Ref. [15]. In light of this, and also considering the very large statistical errors, a firm conclusion about the consistency of our results with heavy-quark scaling laws cannot be drawn.

## V. PHYSICAL RESULTS

In this section, we present a summary of the results obtained in this study, in a form which is easily comparable with the experimental data. All masses are given with an asymmetric statistical error arising from the bootstrap analysis, and a systematic error solely because of the uncertainty in the scale [see Eq. (18)].

In Table II we quote the charm and  $b$ -flavored baryon masses, together with the experimental values, where available. Our results agree well with the experimental data for the charm sector, and also for  $\Lambda_b$  and  $\Sigma_b$ , despite the long extrapolation in the heavy mass scale needed in these cases. This gives us confidence in the reliability of our predictions for the masses of the undiscovered charm and  $b$ -flavored baryons. The quality of the results at the  $b$ -quark mass was certainly enhanced by the number of heavy-quark masses available for this investigation, which allowed us to try dif-

ferent extrapolation procedures and to perform consistency checks. On the other hand, we only have a limited sample of light-quark masses. Although the light extrapolations were always smooth and reasonable, the chiral behavior should be confirmed by using a larger number of light-quark masses.

We present the mass splittings of Sec. IV in Table VII. In those cases where comparison with experiment is possible, we also compute the ratios of the splitting to the sum of the masses, to eliminate most of the uncertainty in the scale. These results were presented in the Introduction, see Eqs. (1)–(4). The residual systematic uncertainty, which is always smaller than the statistical error, was not quoted.

In those cases where a meaningful comparison with experiment is possible, the agreement is very encouraging. Unfortunately, the mass differences, being small, are affected by large relative errors varying between 10 and 30%. Nevertheless, we stress the beautiful agreement with the experimental data, both at the charm and at the  $b$ -quark mass. In particular, in our calculation of the  $\Lambda_b$ -pseudoscalar meson splitting, the agreement with experiment has significantly improved on previous calculations, performed with the standard Wilson action. We believe that this success is further evidence of the advantages of using the Sheikholeslami-Wohlert fermion action.

## VI. CONCLUSIONS

In this paper we have presented the result of a lattice study of heavy baryon spectroscopy. The spectrum of the

TABLE VIII. Estimates of  $M_{\Sigma^*} - M_{\Sigma}$  in lattice units at various masses, obtained by taking the difference of the fitted masses, in lattice units. The extrapolations are linear, following the same procedure adopted for the other splittings.

$\kappa_{l1}/\kappa_{l2}$	$\kappa_h = 0.121$	$\kappa_h = 0.125$	$\kappa_h = 0.129$	$\kappa_h = 0.133$
0.14144/0.14144	(-0.53 +17 -28) $\times 10^{-2}$	(-0.60 +18 -30) $\times 10^{-2}$	(-0.74 +21 -34) $\times 10^{-2}$	(-0.93 +22 -41) $\times 10^{-2}$
0.14144/0.14226	(-0.50 +18 -39) $\times 10^{-2}$	(-0.58 +23 -42) $\times 10^{-2}$	(-0.67 +21 -49) $\times 10^{-2}$	(-0.85 +24 -58) $\times 10^{-2}$
0.14226/0.14226	(-0.49 +26 -57) $\times 10^{-2}$	(-0.63 +31 -62) $\times 10^{-2}$	(-0.68 +32 -68) $\times 10^{-2}$	(-0.84 +38 -78) $\times 10^{-2}$
Strange/strange	(-0.50 +19 -41) $\times 10^{-2}$	(-0.58 +23 -43) $\times 10^{-2}$	(-0.66 +22 -52) $\times 10^{-2}$	(-0.86 +26 -61) $\times 10^{-2}$
Chiral/strange	(-0.40 +36 -75) $\times 10^{-2}$	(-0.50 +45 -85) $\times 10^{-2}$	(-0.63 +48 -86) $\times 10^{-2}$	(-0.97 +56 -94) $\times 10^{-2}$
Chiral/chiral	(-0.42 +41 -90) $\times 10^{-2}$	(-0.55 +48 -92) $\times 10^{-2}$	(-0.43 +40 -110) $\times 10^{-2}$	(-0.64 +49 -126) $\times 10^{-2}$

TABLE IX. Estimates of  $\alpha$  and  $Z_S^2$  from the fitted values of  $Z_m, Z_E, Z_p$ . In the second row corresponding to each  $\kappa_h$ , the fitted  $Z_m$  and  $Z_E$  are compared with the estimates using Eq. (32), and the measured values of  $Z_S^2$  and  $\alpha$ .

$$\text{Momentum } \vec{p} = \left( \frac{2\pi}{L}, 0, 0 \right)$$

	$Z_E^2$	$Z_m^2$	$Z_p^2$	$Z_T^2$	$\alpha$
$\kappa_h = 0.121$	$(2.84 \begin{smallmatrix} +40 \\ -37 \end{smallmatrix}) \times 10^4$	$(2.80 \begin{smallmatrix} +41 \\ -36 \end{smallmatrix}) \times 10^4$	$(1.86 \begin{smallmatrix} +17 \\ -14 \end{smallmatrix}) \times 10^4$	$(2.82 \begin{smallmatrix} +41 \\ -37 \end{smallmatrix}) \times 10^4$	$0.66 \begin{smallmatrix} +6 \\ -7 \end{smallmatrix}$
	$(2.80 \begin{smallmatrix} +40 \\ -36 \end{smallmatrix}) \times 10^4$	$(2.84 \begin{smallmatrix} +41 \\ -37 \end{smallmatrix}) \times 10^4$			
$\kappa_h = 0.125$	$(2.86 \begin{smallmatrix} +43 \\ -38 \end{smallmatrix}) \times 10^4$	$(2.79 \begin{smallmatrix} +44 \\ -37 \end{smallmatrix}) \times 10^4$	$(1.99 \begin{smallmatrix} +18 \\ -15 \end{smallmatrix}) \times 10^4$	$(2.83 \begin{smallmatrix} +44 \\ -38 \end{smallmatrix}) \times 10^4$	$0.71 \begin{smallmatrix} +7 \\ -7 \end{smallmatrix}$
	$(2.81 \begin{smallmatrix} +42 \\ -37 \end{smallmatrix}) \times 10^4$	$(2.85 \begin{smallmatrix} +44 \\ -38 \end{smallmatrix}) \times 10^4$			
$\kappa_h = 0.129$	$(2.83 \begin{smallmatrix} +35 \\ -30 \end{smallmatrix}) \times 10^4$	$(2.73 \begin{smallmatrix} +33 \\ -29 \end{smallmatrix}) \times 10^4$	$(2.17 \begin{smallmatrix} +20 \\ -17 \end{smallmatrix}) \times 10^4$	$(2.78 \begin{smallmatrix} +34 \\ -30 \end{smallmatrix}) \times 10^4$	$0.78 \begin{smallmatrix} +7 \\ -7 \end{smallmatrix}$
	$(2.76 \begin{smallmatrix} +34 \\ -29 \end{smallmatrix}) \times 10^4$	$(2.80 \begin{smallmatrix} + \\ - \end{smallmatrix}) \times 10^4$			
$\kappa_h = 0.133$	$(2.77 \begin{smallmatrix} +35 \\ -32 \end{smallmatrix}) \times 10^4$	$(2.62 \begin{smallmatrix} +34 \\ -29 \end{smallmatrix}) \times 10^4$	$(2.29 \begin{smallmatrix} +22 \\ -17 \end{smallmatrix}) \times 10^4$	$(2.69 \begin{smallmatrix} +36 \\ -30 \end{smallmatrix}) \times 10^4$	$0.85 \begin{smallmatrix} +8 \\ -7 \end{smallmatrix}$
	$(2.68 \begin{smallmatrix} +35 \\ -28 \end{smallmatrix}) \times 10^4$	$(2.71 \begin{smallmatrix} +36 \\ -32 \end{smallmatrix}) \times 10^4$			

$$\text{Momentum } \vec{p} = \left( \frac{2\pi}{L}, \frac{2\pi}{L}, 0 \right)$$

	$Z_E^2$	$Z_m^2$	$Z_p^2$	$Z_T^2$	$\alpha$
$\kappa_h = 0.121$	$(1.94 \begin{smallmatrix} +28 \\ -35 \end{smallmatrix}) \times 10^4$	$(1.93 \begin{smallmatrix} +36 \\ -28 \end{smallmatrix}) \times 10^4$	$(1.09 \begin{smallmatrix} +14 \\ -11 \end{smallmatrix}) \times 10^4$	$(1.94 \begin{smallmatrix} +28 \\ -36 \end{smallmatrix}) \times 10^4$	$0.56 \begin{smallmatrix} +11 \\ -7 \end{smallmatrix}$
	$(1.90 \begin{smallmatrix} +27 \\ -35 \end{smallmatrix}) \times 10^4$	$(1.97 \begin{smallmatrix} +29 \\ -37 \end{smallmatrix}) \times 10^4$			
$\kappa_h = 0.125$	$(1.93 \begin{smallmatrix} +32 \\ -33 \end{smallmatrix}) \times 10^4$	$(1.91 \begin{smallmatrix} +32 \\ -33 \end{smallmatrix}) \times 10^4$	$(1.16 \begin{smallmatrix} +15 \\ -12 \end{smallmatrix}) \times 10^4$	$(1.92 \begin{smallmatrix} +32 \\ -33 \end{smallmatrix}) \times 10^4$	$0.61 \begin{smallmatrix} +12 \\ -8 \end{smallmatrix}$
	$(1.89 \begin{smallmatrix} +31 \\ -32 \end{smallmatrix}) \times 10^4$	$(1.96 \begin{smallmatrix} +32 \\ -34 \end{smallmatrix}) \times 10^4$			
$\kappa_h = 0.129$	$(1.93 \begin{smallmatrix} +32 \\ -33 \end{smallmatrix}) \times 10^4$	$(1.88 \begin{smallmatrix} +30 \\ -33 \end{smallmatrix}) \times 10^4$	$(1.25 \begin{smallmatrix} +16 \\ -13 \end{smallmatrix}) \times 10^4$	$(1.91 \begin{smallmatrix} +30 \\ -34 \end{smallmatrix}) \times 10^4$	$0.66 \begin{smallmatrix} +14 \\ -9 \end{smallmatrix}$
	$(1.87 \begin{smallmatrix} +29 \\ -31 \end{smallmatrix}) \times 10^4$	$(1.95 \begin{smallmatrix} +32 \\ -35 \end{smallmatrix}) \times 10^4$			
$\kappa_h = 0.133$	$(1.89 \begin{smallmatrix} +32 \\ -34 \end{smallmatrix}) \times 10^4$	$(1.79 \begin{smallmatrix} +32 \\ -32 \end{smallmatrix}) \times 10^4$	$(1.34 \begin{smallmatrix} +18 \\ -14 \end{smallmatrix}) \times 10^4$	$(1.84 \begin{smallmatrix} +32 \\ -33 \end{smallmatrix}) \times 10^4$	$0.73 \begin{smallmatrix} +16 \\ -10 \end{smallmatrix}$
	$(1.80 \begin{smallmatrix} +31 \\ -30 \end{smallmatrix}) \times 10^4$	$(1.88 \begin{smallmatrix} +34 \\ -36 \end{smallmatrix}) \times 10^4$			

eight lowest-lying heavy baryons, containing a single heavy quark, can be computed using the three baryonic operators in Eq. (5). In addition to the calculation of the  $\Lambda$  and  $\Xi$  masses, we have discussed how to compute the spectrum of the spin doublets,  $(\Sigma, \Sigma^*)$ ,  $(\Xi', \Xi^*)$ , and  $(\Omega, \Omega^*)$ , by isolating their contributions to the correlation functions of the operators  $\mathcal{O}_\mu$  and  $\mathcal{O}'_\mu$ .

The computation of the mass spectrum proved feasible; the operators we have used have a good overlap with various baryon ground states, in part thanks to the smearing both at the source and at the sink. Moreover, the extrapolations in both the heavy- and light-quark masses are always smooth. The agreement between our estimates of the baryon masses and the experimental values is good, in both the charm and the  $b$ -quark sectors.

The computed  $\Lambda$ -pseudoscalar meson mass splitting is in good agreement with experiment, in contrast with the results of previous calculations performed with the Wilson fermion action. We believe that this is largely because of the use of the  $O(a)$ -improved action to remove systematic effects. A similar positive conclusion can be drawn for the  $\Sigma$ - $\Lambda$  splitting, although the statistical errors are still of the order of 25–30%.

Our results are also in agreement with the predictions ob-

tained with other nonperturbative methods [7–9], both for the masses themselves and for the  $\Sigma$ - $\Lambda$  splitting. In the case of the  $\Xi'$ - $\Xi$  splitting, which is of the same nature as the  $\Sigma$ - $\Lambda$  splitting, the calculation is complicated by the mixing arising between the two particles, whose total quantum numbers are the same. It has been noted [9] that such a mixing, negligible in the heavy-quark limit, would have the effect of increasing the splitting. Both our prediction and that of Savage [9] are higher than those of the experiment [12]. The disagreement would, hence, get even worse if we were to take the mixing into account. We stress, anyway, that this experimental result is still to be confirmed.

In this exploratory study, the masses have been determined with reasonable precision, but further studies are required to reduce both the statistical and systematic errors. The results presented in this paper are very encouraging and it looks likely that it will also be possible to measure the baryonic matrix elements.

#### ACKNOWLEDGMENTS

The authors wish to thank Robert Coquereaux, Oleg Ogievetsky, Jay Watson, and Jonathan Flynn for helpful discussions. This research was supported by the U.K. Science

TABLE X. Values of  $Z_l = (Z_l Z_s) / \sqrt{Z_s^2}$ , for the four heavy masses and  $\kappa_{l1} = \kappa_{l2} = 0.14144$ .

Momentum	$\kappa_h = 0.121$	$\kappa_h = 0.125$	$\kappa_h = 0.129$	$\kappa_h = 0.133$
$\vec{p} = \vec{0}$	$(3.8 \begin{smallmatrix} +4 \\ -3 \end{smallmatrix}) \times 10^{-3}$	$(3.6 \begin{smallmatrix} +3 \\ -3 \end{smallmatrix}) \times 10^{-3}$	$(3.5 \begin{smallmatrix} +3 \\ -3 \end{smallmatrix}) \times 10^{-3}$	$(3.2 \begin{smallmatrix} +3 \\ -2 \end{smallmatrix}) \times 10^{-3}$
$\vec{p} = (\frac{2\pi}{L}, 0, 0)$	$(3.9 \begin{smallmatrix} +4 \\ -4 \end{smallmatrix}) \times 10^{-3}$	$(3.7 \begin{smallmatrix} +4 \\ -4 \end{smallmatrix}) \times 10^{-3}$	$(3.6 \begin{smallmatrix} +4 \\ -3 \end{smallmatrix}) \times 10^{-3}$	$(3.3 \begin{smallmatrix} +4 \\ -3 \end{smallmatrix}) \times 10^{-3}$
$\vec{p} = (\frac{2\pi}{L}, \frac{2\pi}{L}, 0)$	$(3.8 \begin{smallmatrix} +5 \\ -4 \end{smallmatrix}) \times 10^{-3}$	$(3.7 \begin{smallmatrix} +5 \\ -4 \end{smallmatrix}) \times 10^{-3}$	$(3.5 \begin{smallmatrix} +5 \\ -4 \end{smallmatrix}) \times 10^{-3}$	$(3.3 \begin{smallmatrix} +5 \\ -4 \end{smallmatrix}) \times 10^{-3}$

and Engineering Research Council under Grant No. GR/G 32779, by the Particle Physics and Astronomy Research Council under Grant No. GR/J 21347, by the European Union under Contract No. CHRX-CT92-0051, by the University of Edinburgh, and by Meiko Limited. C.T.S. and D.G.R. acknowledge the support of the Particle Physics and Astronomy Research Council. N.S. thanks the University of Rome ‘‘La Sapienza’’ for financial support. J.N. and P.U. acknowledge the European Union for their support through Contract Nos. CHBICT920066 and CHBICT930877. O.O. was supported by JNICT under Grant No. BD/2714/93.

#### APPENDIX: EFFECT OF SMEARING ON BARYON CORRELATION FUNCTIONS

In this appendix we propose a description of the effect of a non-Lorentz-invariant smearing on a nonscalar operator. Interpolating operators are smeared to improve their overlap with the physical states one wishes to create or annihilate. We discuss the case of two-point correlation functions, restricting ourselves to the case of spinorial operators which have an overlap with a single type of spin- $\frac{1}{2}$  particle, such as  $\mathcal{O}_5(x)$  defined in Eq. (5). Numerical evidence for this effect is also presented. It should be noted that the breaking of the Lorentz symmetry manifests itself only when one considers correlators at finite momentum, and has, therefore, no relevance to the determination of the spectrum.

Let us write the general expression for a local baryonic operator,

$$J_\rho(x) = [\psi(x)\Gamma\psi(x)]\psi_\rho(x), \quad (\text{A1})$$

and consider the case where it has an overlap with spin- $\frac{1}{2}$  states, such as  $\mathcal{O}_5$ . It can destroy one such state, according to the relation

$$\langle 0|J_\rho(0)|\vec{p}, r\rangle = Zu^{(r)}(\vec{p}). \quad (\text{A2})$$

In Eqs. (26) and (27),  $\rho$  and  $r$  are the spinorial and polarization indices, respectively, the antisymmetric sum over color is understood, and  $\Gamma$  is a suitable combination of gamma and charge conjugation matrices. Finally, the amplitude  $Z$  is a Lorentz scalar.

In general, a smeared baryonic operator can be written as

$$J_\rho^s(\vec{x}, t) = \sum_{y,z,w} f(|\vec{y}-\vec{x}|)f(|\vec{z}-\vec{x}|)f(|\vec{w}-\vec{x}|) \times [\psi(\vec{y}, t)\Gamma\psi(\vec{z}, t)]\psi_\rho(\vec{w}, t). \quad (\text{A3})$$

Because the smearing is performed only in the spatial directions, Lorentz symmetry is lost and only spatial translations, rotations, parity, and time reversal survive. Therefore, the overlap of the operator  $J_\rho^s(\vec{x}, t)$  with the state  $|\vec{p}, r\rangle$  is given by the more general expression

$$\langle 0|J_\rho^s(0)|\vec{p}, r\rangle = [Z_1(|\vec{p}|)u^{(r)}(\vec{p}) + Z_2(|\vec{p}|)\gamma_0 u^{(r)}(\vec{p})]_\rho, \quad (\text{A4})$$

where the amplitudes  $Z_1$  and  $Z_2$  may depend on the magnitude of the three-momentum of the state  $|\vec{p}, r\rangle$ , in accord with the restricted symmetries of the system.

Let us consider the case of an SS two-point correlator, for large  $t$ :

$$\begin{aligned} G_{\rho\sigma}^{ss}(t, \vec{p}) &= \sum_x \langle 0|T[J_\rho^s(\vec{x}, t)\bar{J}_\sigma^s(\vec{0}, 0)]|0\rangle e^{-i\vec{p}\cdot\vec{x}} \\ &= \sum_{|\vec{q}, r} \sum_x \frac{m}{E(\vec{p})} \langle 0|J_\rho^s(\vec{0}, 0)|\vec{q}, r\rangle \\ &\quad \times \langle \vec{q}, r|\bar{J}_\sigma^s(\vec{0}, 0)|0\rangle e^{-i\vec{p}\cdot\vec{x}} e^{i\vec{q}\cdot\vec{x}} \\ &= \sum_r \frac{m e^{-E(\vec{p})t}}{E(\vec{p})} \{ [Z_1(|\vec{p}|) + Z_2(|\vec{p}|)\gamma_0] u^{(r)}(\vec{p}) \bar{u}^{(r)} \\ &\quad \times (\vec{p}) [Z_1(|\vec{p}|) + Z_2(|\vec{p}|)\gamma_0] \}_{\rho\sigma}. \end{aligned} \quad (\text{A5})$$

This expression can be conveniently rewritten as

$$\begin{aligned} G_{\rho\sigma}^{ss}(t, \vec{p}) &= Z_s^2(|\vec{p}|) e^{-E(\vec{p})t} \left[ \frac{E+m-\alpha^2(E-m)}{4E} \mathbb{1} \right. \\ &\quad \left. + \frac{E+m+\alpha^2(E-m)}{4E} \gamma_0 - \frac{2\alpha}{4E} \vec{p}\cdot\vec{\gamma} \right]_{\rho\sigma}, \end{aligned} \quad (\text{A6})$$

where  $Z_s = Z_1 + Z_2$ ,  $\alpha = (Z_1 - Z_2)/(Z_1 + Z_2)$ , and full Lorentz symmetry is recovered when  $\alpha = 1$ . Equation (31) exhibits the following features: the exponential falloff is not altered by the smearing. This was expected since a smearing function, which only extends in the spatial directions, preserves the form of the transfer matrix; it has the correct limit

for  $\alpha \rightarrow 1$ :  $G^{ss}(\vec{p}, t) \propto G^{\text{loc}}(\vec{p}, t)$ ; the degeneracy among the amplitudes of different spinorial components of the correlator is lifted; and all the terms proportional to  $\alpha$  vanish for  $\vec{p} \rightarrow \vec{0}$ , so that the effect disappears at zero momentum.<sup>5</sup>

In the following, we will check this effect against the numerical data. It is convenient to rewrite Eq. (31) in the form

$$G^{ss}(\vec{p}, t) = \frac{e^{-E(\vec{p})t}}{2E} \{mZ_m + \gamma_0 E Z_E - \vec{p} \cdot \vec{\gamma} Z_p\}, \quad \text{with} \quad \begin{cases} Z_E = [E + m + \alpha^2(E - m)] \frac{Z_s^2}{2E}, \\ Z_m = [E + m - \alpha^2(E - m)] \frac{Z_s^2}{2m}, \\ Z_p = \alpha Z_s^2. \end{cases} \quad (\text{A7})$$

We have found that  $Z_E$  and  $Z_m$  are compatible, as they should be, considering that they differ by terms proportional to  $\vec{p}^2/Em$ , which are very small for the values of momenta and masses in our simulation. Furthermore,  $Z_p$  is significantly different from  $Z_E$  and  $Z_m$ , which shows that  $\alpha$  is different from one.  $Z_s$  and  $\alpha$  are given by

$$Z_s^2 = \frac{EZ_E + mZ_m}{E + m} \quad (\text{A8})$$

and

$$\alpha = \frac{Z_p}{Z_s^2}.$$

The results of this exercise are presented in Table IX for the  $\Lambda$  baryon with momentum  $\vec{p} = (2\pi/L, 0, 0)$  and  $(2\pi/L, 2\pi/L, 0)$ , for masses corresponding to the four values of  $\kappa_h$  and  $\kappa_{l1} = \kappa_{l2} = 0.14144$ . Using the estimated values of  $Z_s^2$  and  $\alpha$ , we have also recomputed  $Z_E$  and  $Z_m$  (second row

of Table IX) and verified that they are compatible with the fitted values. The numerical results are consistent with the picture illustrated above, and the value of  $\alpha$  is significantly different from 1, demonstrating that such an effect cannot be neglected.

We conclude this appendix with a discussion of the SL correlators, whose spin structure is again different from that of local correlators. This feature must be taken into account in the analysis of three-point correlators when the inserted current operator is local. Following the reasoning above, we find

$$G^{sl}(t, \vec{p}) = Z_l Z_s(|\vec{p}|) e^{-E(\vec{p})t} \left\{ \frac{E + m - \alpha(E - m)}{4E} \right. \\ \left. + \frac{E + m + \alpha(E - m)}{4E} \gamma_0 \right. \\ \left. - \frac{(1 + \gamma_0) + \alpha(1 - \gamma_0)}{4E} \vec{p} \cdot \vec{\gamma} \right\}. \quad (\text{A9})$$

As above, it is possible to measure  $Z_s Z_l$  averaging  $Z_E$  and  $Z_m$ . By doing so, we have extracted  $Z_l$  for three different values of the momentum, and the results are shown in Table X. The evidence that  $Z_l$  is independent of  $\vec{p}$  is a further check of the validity of our interpretation.

<sup>5</sup>For this reason, this effect has no consequences for the results presented in this paper.

- [1] C. Albajar *et al.*, Phys. Lett. B **273**, 540 (1991); G. Bari *et al.*, Nuovo Cimento A **104**, 1787 (1991).  
 [2] ALEPH Collaboration, D. Decamp *et al.*, Phys. Lett. B **278**, 367 (1992); OPAL Collaboration, P. Acton *et al.*, *ibid.* **281**, 394 (1992); ALEPH Collaboration, D. Buskulic *et al.*, *ibid.* **294**, 145 (1992); DELPHI Collaboration, P. Abreu *et al.*, *ibid.* **311**, 379 (1993).  
 [3] S. F. Biagi *et al.*, Z. Phys. C **28**, 175 (1985); ARGUS Collaboration, H. Albrecht *et al.*, Phys. Lett. B **288**, 367 (1992); Fermilab E687 Collaboration, P. L. Frabetti *et al.*, *ibid.* **300**, 190 (1993); **338**, 106 (1994); contribution to LISHEP95, Rio de

- Janeiro, 1995 (unpublished); CERN WA89 Collaboration, M. I. Adamovich *et al.*, Phys. Lett. B **358**, 151 (1991), and references therein.

- [4] Several contributions at the EPS HEP-95 Conference focused on this topic: DELPHI Collaboration, DELPHI-95-107, Contribution No. eps0565, Brussel, 1995 (unpublished).  
 [5] For a review, see, e.g., M. Neubert, Phys. Rep. **245**, 245 (1994).  
 [6] J.G. Körner, D. Pirjol, and M. Krämer, Prog. Part. Nucl. Phys. **33**, 787 (1994).  
 [7] A. De Rújula, H. Georgi, and S.L. Glashow, Phys. Rev. D **12**,

- 147 (1975); A. Martin and J. M. Richard, Phys. Lett. B **185**, 426 (1987), and references therein.
- [8] J. L. Rosner, Phys. Rev. D **52**, 6461 (1995); R. Roncaglia, D. B. Lichtenberg, and E. Predazzi, *ibid.* **53**, 6678 (1996).
- [9] M. J. Savage, Phys. Lett. B **359**, 189 (1995); see also M. K. Banerjee and J. Milana, Phys. Rev. D **52**, 6451 (1995).
- [10] UKQCD Collaboration, N. Stella, in *Lattice '94*, Proceedings of the International Symposium, Bielefeld, Germany, edited by F. Karsch *et al.* [Nucl. Phys. B (Proc. Suppl.) **42**, 367 (1995); C. Alexandrou *et al.*, *ibid.*, p. 297.
- [11] C. Alexandrou *et al.*, Phys. Lett. B **337**, 340 (1994).
- [12] WA89 Collaboration, P. Avery *et al.*, Phys. Rev. Lett. **75**, 4364 (1995).
- [13] J. L. Rosner, Prog. Theor. Phys. **66**, 1422 (1981).
- [14] UKQCD Collaboration, C. R. Allton *et al.*, Phys. Lett. B **292**, 408 (1992).
- [15] A. S. Kronfeld and P. B. Mackenzie, Annu. Rev. Nucl. Part. Sci. **43**, 793 (1993).
- [16] G. P. Lepage and P. B. Mackenzie, Phys. Rev. D **48**, 2250 (1993); UKQCD Collaboration (work in progress).
- [17] Particle Data Group, L. Montanet *et al.*, Phys. Rev. D **50**, 1173 (1994).
- [18] SKAT Collaboration, V. V. Ammosov *et al.*, in *Lepton and Photon Interactions*, Proceedings of the XVI International Symposium, Ithaca, New York, 1993, edited by P. Drell and D. Rubin, AIP Conf. Proc. No. 302 (AIP, New York, 1994).
- [19] UKQCD Collaboration, C. R. Allton *et al.*, Nucl. Phys. **B407**, 331 (1993).
- [20] M. Benmerrouche *et al.*, Phys. Rev. C **39**, 2339 (1989).
- [21] W. Rarita and J. Schwinger, Phys. Rev. **60**, 61 (1941).
- [22] D. Lurie, *Particles and Fields* (Interscience, New York, 1968).
- [23] B. Sheikholeslami and R. Wohlert, Nucl. Phys. **B259**, 572 (1985).
- [24] G. Heatlie, C. T. Sachrajda, G. Martinelli, C. Pittori, and G. C. Rossi, Nucl. Phys. **B352**, 266 (1991).
- [25] UKQCD Collaboration, C. R. Allton *et al.*, Phys. Rev. D **49**, 474 (1994).
- [26] R. Gupta, in *Lattice '95*, Proceedings of the International Symposium, Melbourne, Australia, edited by T. D. Kiev *et al.* [Nucl. Phys. B (Proc. Suppl.) **47** (1996)], Report No. hep-lat/9512021 (unpublished).
- [27] R. Sommer, Nucl. Phys. **B411**, 839 (1994); G. de Divitiis *et al.*, *ibid.* **B437**, 447 (1994).
- [28] UKQCD Collaboration, H. Wittig, in *Lattice '94* [10], p. 288.
- [29] UKQCD Collaboration, D. S. Henty *et al.*, Phys. Rev. D **51**, 5323 (1995).
- [30] UKQCD Collaboration, C. R. Allton *et al.* Phys. Rev. D **47**, 5128 (1993).
- [31] M. Bochicchio, G. Martinelli, C. R. Allton, C. T. Sachrajda, and D. B. Carpenter, Nucl. Phys. **B372**, 403 (1992).
- [32] UKQCD Collaboration, A. K. Ewing, Nucl. Phys. (Proc. Suppl.) **B42**, 331 (1995).
- [33] UKQCD Collaboration, A. K. Ewing *et al.*, this issue, Phys. Rev. D **54**, 3526 (1996).
- [34] UKQCD Collaboration, R. M. Baxter *et al.*, Phys. Rev. D **49**, 1594 (1994).
- [35] J. E. Mandula and E. Shpiz, Nucl. Phys. **B232**, 180 (1984).
- [36] L. C. Chen and J. L. Birman, J. Math. Phys. **12**, 2454 (1971).
- [37] J. E. Mandula, G. Zweig, and J. Govaerts, Nucl. Phys. **B228**, 91 (1983); **B228**, 109 (1983).